Supporting Information

Extending Molecular Conjugation of Phosphorescence Units to Accurately Modulate Ultralong Organic Room Temperature Phosphorescence

Jingjuan Bai,[a] Guangkuo Dai,[a] Huiwen Jin,[a] Jiaxin Ma,[a] Zewei Li,[b] Yan Guan,[b] Mingxing Chen,[b] Zhimin Ma[b] and Zhiyong Ma[a]*

[a] Prof. Z.Y. Ma, Miss. J.J. Bai, Mr. G.K. Dai, Miss H.W. Jin, Miss J.X. Ma
Beijing Advanced Innovation Center for Soft Matter Science and Engineering, State Key Laboratory of Organic-Inorganic Composites, College of Chemical Engineering, Beijing University of Chemical Technology, Beijing 100029, China. E-mail: mazhy@mail.buct.edu.cn.

[b] *Dr. Z.M. Ma, Dr. Y. Guan, Mr. M.X. Chen, Mr. Z.W. Li*
College of Engineering, Peking University, Beijing 100871, China.

Supporting information for this article is given via a link at the end of the document.

Jingjuan Bai and Guangkuo Dai contributed equally.

Table of Contents

1. Materials and General Methods

All the solvents and reactants were purchased from commercialized companies and used as received without further purification except for specifying otherwise.

^{1}H NMR was recorded on the 400 MHz (Bruker ARX400) and ^{13}C NMR spectra were recorded on the Bruker 101 MHz spectrometer at room temperature with $CDCl_3$ and DMSO-d_6 as the solvents and tetramethylsilane (TMS) as the internal standard. ESI high resolution mass-spectra (HRMS) were acquired on a Waters Xevo G2 Qt of mass spectrometer. Transient and delayed photoluminescence spectra were performed on the Hitachi F-4600 or Edinburgh Instruments FLS1000 fluorescence spectrophotometer. Luminescence lifetime were acquired on the Edinburgh Instruments FLS1000 fluorescence spectrophotometer or Deltaflex Fluorescence Lifetime Instrument (λ_{ex}=365 nm). The lifetimes are fitted with the software that comes with the Edinburgh Instruments FLS1000 instrument to give the appropriate order of fit. The program uses a double exponential function fit. The lifetime fitting equation is $\tau=(B_1\tau 2\ 1+B_2\tau 2\ 2)/(B_1\tau_1+B_2\tau_2)$. Single crystal X-ray diffraction data were collected with a NONIUS KappaCCD diffractometer with graphite monochromator and Mo Kα radiation [λ (MoKα) = 0.71073 Å]. Structures were solved by direct methods with SHELXS-97 and refined against F2 with SHELXS-97. Single crystals of $C_{22}H_{13}N$ were recrystallised from organic solvent mounted in inert oil and transferred to the cold gas stream of the diffractometer.

TD-DFT calculations were conducted on Gaussian 09 program with a method similar to previous literature.[1] Ground state (S_0) geometries of PyCz and BrPyCz monomer were directly optimized in vacuum condition. On the basis of this, exciton energies in singlet (S_n) and triplet states (T_n) were estimated through a combination of TDDFT and B3LYP at the 6-311+G (p, d) level. We have to emphasize that the computed singlet and triplet levels in this article refer to emission (excited state optimization). Kohn-Sham frontier orbital analysis was subsequently performed based on the results of theoretical calculation to elucidate the mechanisms of possible singlet-triplet intersystem crossings, in which the channels from S_1 to T_n were believed to share part of the same transition orbital compositions. Herein, energy levels of the possible T_n states were considered to lie within the range of ES_1±0.3 eV.[2] Spin-orbital couplings (SOC) matrix elements were conducted through the Beijing Density Functional (BDF) program based on optimized or single crystal structures at the B3LYP/6- 311G* level.

Preparation of Doped PMMA Films: A mixture powder of PMMA (200 mg) and (Br)PyCz (2 mg) was dissolved in dichloromethane (1.5 mL) at room temperature and ultrasonicated at room temperature for 30 min. Then the solution was poured into a prepared culture dish and dried for 30 minutes at ambient condition. As the solvent was completely removed, a

transparent film was obtained. Similarly, the BCz-1 and BCz-2 films were obtained by this method. Preparation of Doped PVA Film: PyCz (0.2 mg) was dissolved in DMSO (2 ml) and ultrasonicated at 50 °C for 30 min, then added to 4.0 ml of PVA (200 mg) aqueous solution, which was stirred at 100 °C for 30 min. The obtained solutions were then ultrasonicated at 60 °C for 1 h to complete the doping process. Dropping the solutions into a prepared culture dish and keeping it at 70 °C for 8 h produced a transparent film. The films were made in the same culture dish, so all samples are comparable in thickness and their thickness are 0.12 mm.

2. Syntheses and characterizations

The synthesis method of the substrates (PyCz and BrPyCz) used in this paper are the same as in our previous work.[3,4] The detailed syntheses of PyCz and BrPyCz are shown as follows.

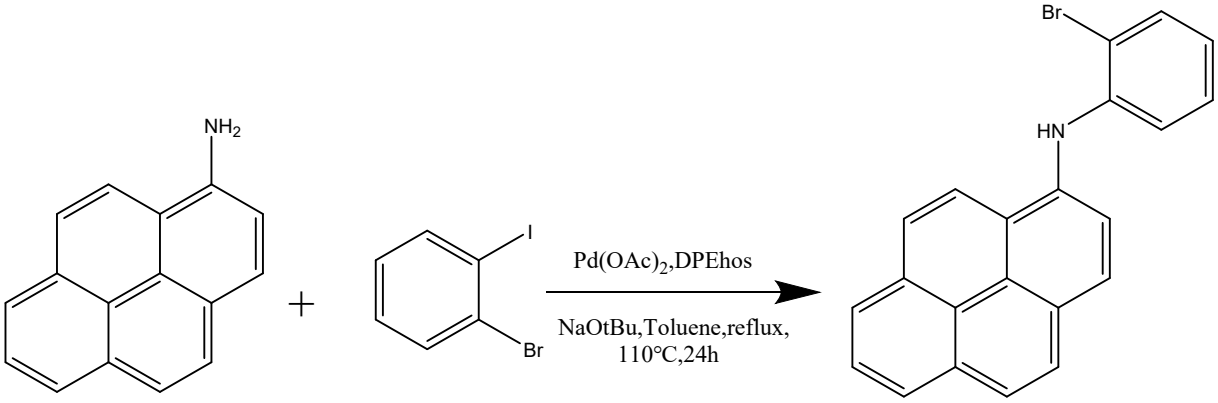

Scheme S1. The synthetic route to N-(2-bromophenyl)pyren-1-amine.

N-(2-bromophenyl)pyren-1-amine: Pyren-1-amine (1.0860 g, 5 mmol), sodium tert-butoxide (720.0 mg, 7.5 mmol), $Pd(OAc)_2$ (25.3 mg, 0.1125 mmol), (oxybis(2,1-phenylene))bis(diphenylphosphine) (61.0 mg, 0.1125 mmol), were added to a 100 mL shrek bottle. Then 1-bromo-2-iodobenzene (1.0600 g, 3.75 mmol) which was dissolved in toluene (10 mL, AR grade) were added to the bottle. The mixed solution was refluxed at 110 ℃ for 24h in nitrogen atmosphere. After the reaction was over, the resultant mixture was cooled down to room temperature and the solvent was removed under reduced pressure. The crude product was purified by silica gel column using petroleum ether as the eluent to obtain pure product as red powder. Yield: 61%.

^{1}H NMR (400 MHz, Chloroform-*d*) δ 8.22 – 8.14 (m, 4H), 8.09 – 7.94 (m, 5H), 7.60 (dd, J = 8.0, 1.5 Hz, 1H), 7.07 (ddd, J = 8.5, 7.2, 1.5 Hz, 1H), 6.85 (dd, J = 8.2, 1.5 Hz, 1H), 6.74 (ddd, J = 7.9, 7.2, 1.5 Hz, 1H), 6.68 (s, 1H).

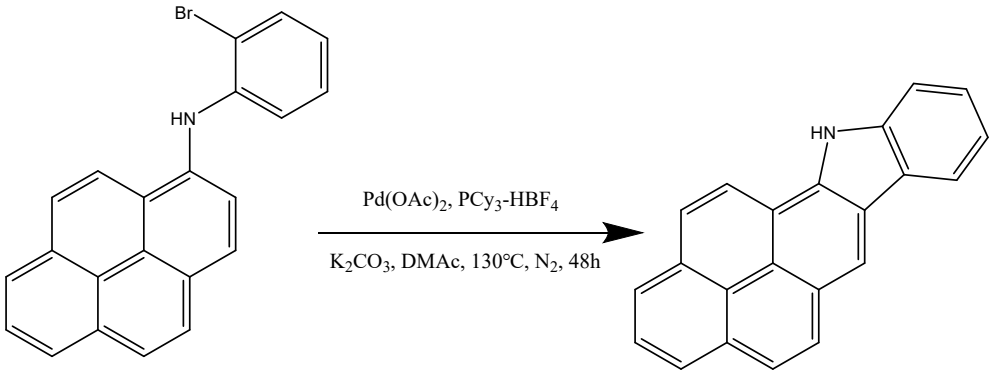

Scheme S2. The synthetic route to PyCz.

PyCz: Potassium carbonate (0.5528 g, 4 mmol), $Pd(OAc)_2$ (13.5 mg, 0.06 mmol), Tricydohexylphosphine tetrafluoroborate (44.2 mg, 0.12 mmol) were added to a 100 mL shrek bottle. Then N-(2-bromophenyl)pyren-1-amine (0.7113 g, 2 mmol) which was dissolved in

DMAC (10 mL, AR grade) was added to the bottle. The mixed solution was refluxed at 130 ℃ for 48h in nitrogen atmosphere. After the reaction was over, the resultant mixture was cooled down to room temperature and the solvent was washed by Saturated brine and DCM for 2 times. The obtained solvent was removed under reduced pressure. The crude product was purified by silica gel column using petroleum ether as the eluent to obtain pure product as yellow powder. Yield: 38%.

^{1}H NMR (400 MHz, DMSO-d_6) δ 12.46 (s, 1H), 9.04 (s, 1H), 8.81 (d, J = 9.0 Hz, 1H), 8.46 (d, J = 7.7 Hz, 1H), 8.32 (d, J = 9.0 Hz, 1H), 8.28 – 8.21 (m, 2H), 8.20 (dd, J = 7.6, 1.1 Hz, 1H), 8.06 – 7.95 (m, 2H), 7.77 (dt, J = 8.0, 0.9 Hz, 1H), 7.58 (ddd, J = 8.2, 7.1, 1.2 Hz, 1H), 7.36 (ddd, J = 8.0, 7.1, 1.0 Hz, 1H)

^{13}C NMR (101 MHz, DMSO-d_6) δ 140.34, 135.12, 131.19, 130.99, 128.57, 126.51, 126.26, 125.75, 125.18, 124.08, 124.01, 123.96, 122.89, 122.78, 121.81, 120.84, 120.74, 119.32, 117.39, 115.04, 111.77.

HR-ESI-MS Calcd. For $C_{22}H_{13}N$ $[M+H]^+$: 292.1128. Found: 292.1107.

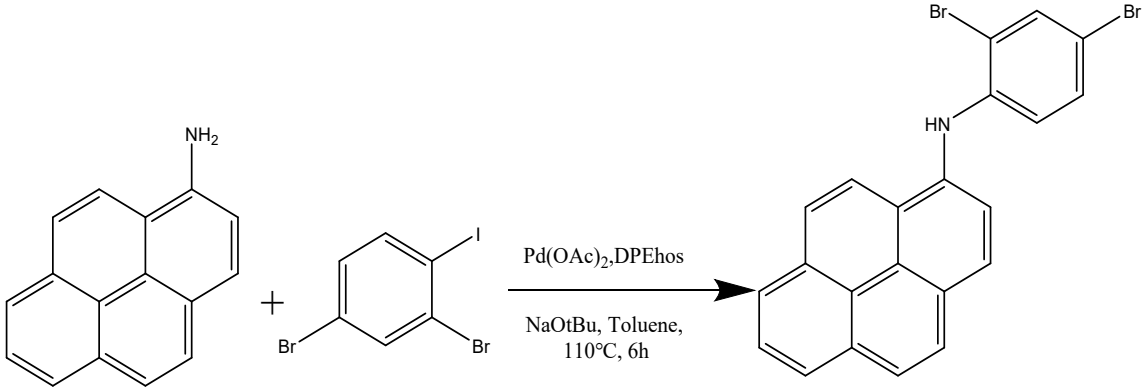

Scheme S3. The synthetic route to N-(2,4-dibromophenyl)pyren-1-amine.

N-(2,4-dibromophenyl)pyren-1-amine: Pyren-1-amine (1.0860 g, 5 mmol), sodium tert-butoxide (720.0 mg, 7.5 mmol), $Pd(OAc)_2$ (25.3 mg, 0.1125 mmol), (oxybis(2,1-phenylene))bis(diphenylphosphine) (61.0 mg, 0.1125 mmol), were added to a 100 mL shrek bottle. Then 2,4-dibromo-1-iodobenzene (1.3568 g, 3.75 mmol) which was dissolved in toluene (10 mL, AR grade) were added to the bottle. The mixed solution was refluxed at 110 ℃ for 6h in nitrogen atmosphere. After the reaction was over, the resultant mixture was cooled down to room temperature and the solvent was removed under reduced pressure. The crude product was purified by silica gel column using petroleum ether as the eluent to obtain pure product as yellow powder. Yield: 37%.

^{1}H NMR (400 MHz, Chloroform-d) δ 8.23 – 8.13 (m, 4H), 8.11 – 7.98 (m, 4H), 7.92 (d, J = 8.2 Hz, 1H), 7.72 (d, J = 2.3 Hz, 1H), 7.14 (dd, J = 2.2 Hz, 1H), 6.64 (d, J = 8.9 Hz, 2H).

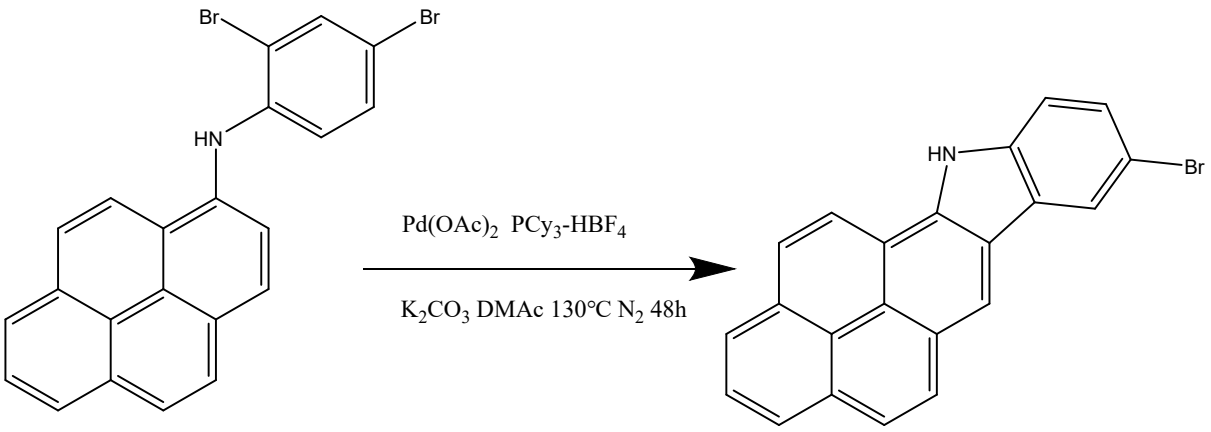

Scheme S4. The synthetic route to BrPyCz.

BrPyCz: Potassium carbonate (0.2749 g, 1.9890 mmol), $Pd(OAc)_2$ (0.0067 mg, 0.0298 mmol), Tricydohexylphosphine tetrafluoroborate (0.022 mg, 0.597 mmol) were added to a 25 mL shrek bottle. Then N-(2,4-dibromophenyl)pyren-1-amine (0.4486 g, 0.9945 mmol) which was dissolved in DMAC (5 mL, AR grade) was added to the bottle. The mixed solution was refluxed at 130 ℃ for 48h in nitrogen atmosphere. After the reaction was over, the resultant mixture was cooled down to room temperature and the solvent was washed by Saturated brine and DCM for 2 times. The obtained solvent was removed under reduced pressure. The crude product was purified by silica gel column using petroleum ether and ethyl acetate as the eluent to obtain pure product as yellow powder. Yield: 41%.

^{1}H NMR (400 MHz, DMSO-d_6) δ 12.64 (s, 1H), 9.10 (s, 1H), 8.80 (d, J = 9.0 Hz, 1H), 8.71 (d, J = 1.9 Hz, 1H), 8.41 – 8.18 (m, 4H), 8.11 – 7.97 (m, 2H), 7.78 – 7.66 (m, 2H).

^{13}C NMR (101 MHz, DMSO-d_6) δ 139.44, 135.91, 131.64, 131.48, 129.01, 128.94, 127.20, 124.82, 123.66, 122.10, 120.25, 118.14, 115.61, 113.73, 111.74.

HR-ESI-MS Calcd. For $C_{22}H_{13}NBr$ $[M+H]^+$: 369.015. Found: 368.980.

3. NMR spectra and HR-MS of mentioned molecules.

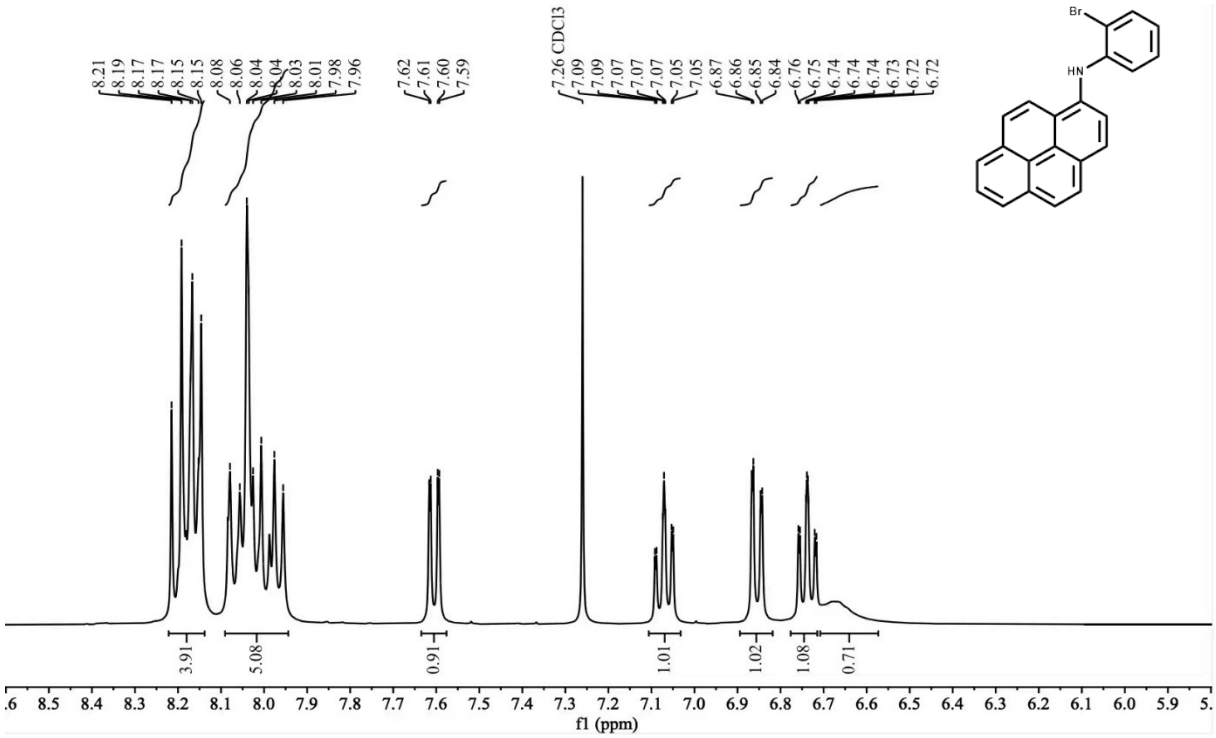

Figure S1. ^{1}H NMR spectrum of N-(2-bromophenyl)pyren-1-amine in Chloroform-*d*.

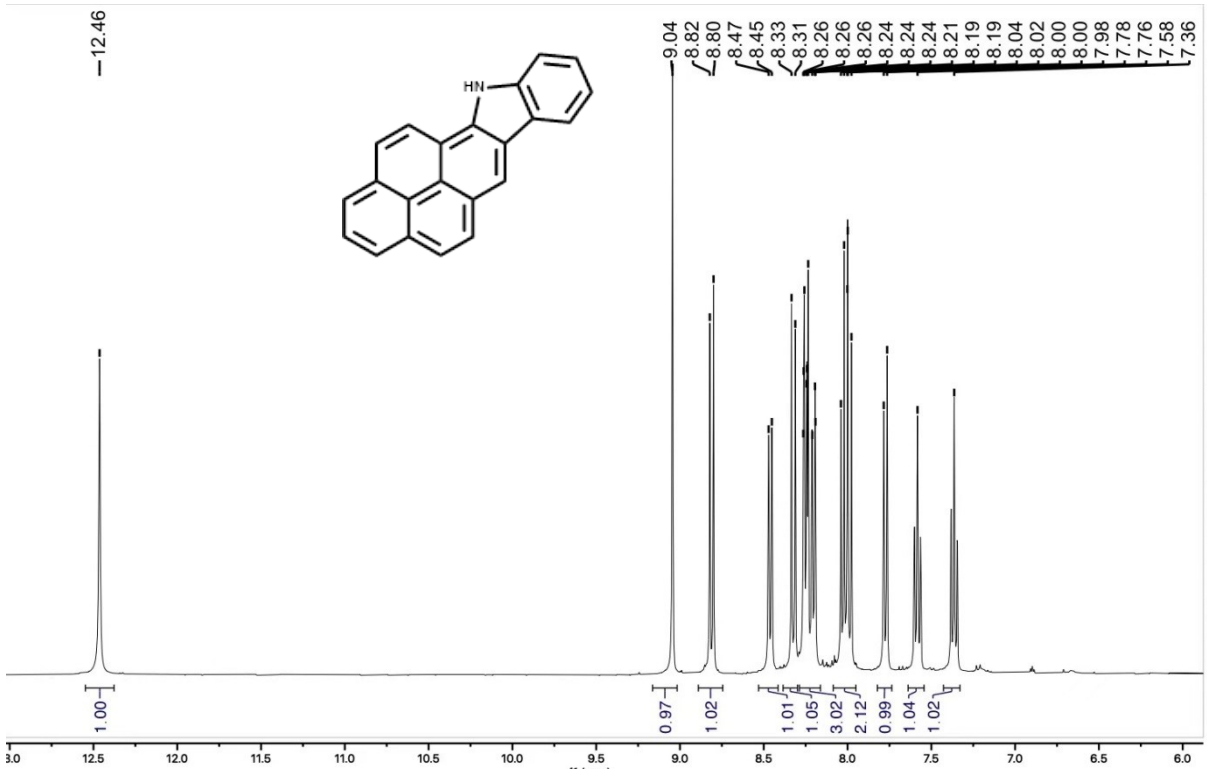

Figure S2. ^{1}H NMR spectrum of PyCz in DMSO-d_6.

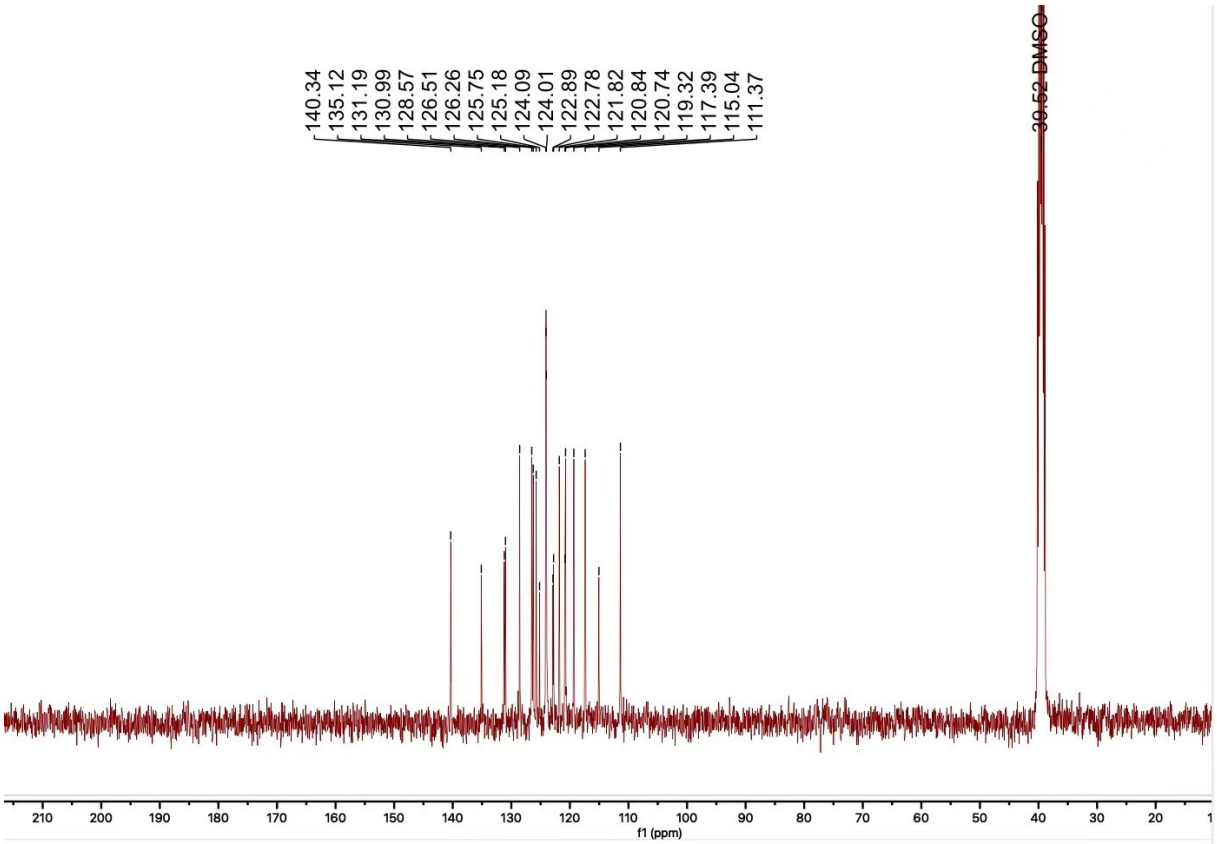

Figure S3. ^{13}C NMR spectrum of PyCz in DMSO-d_6.

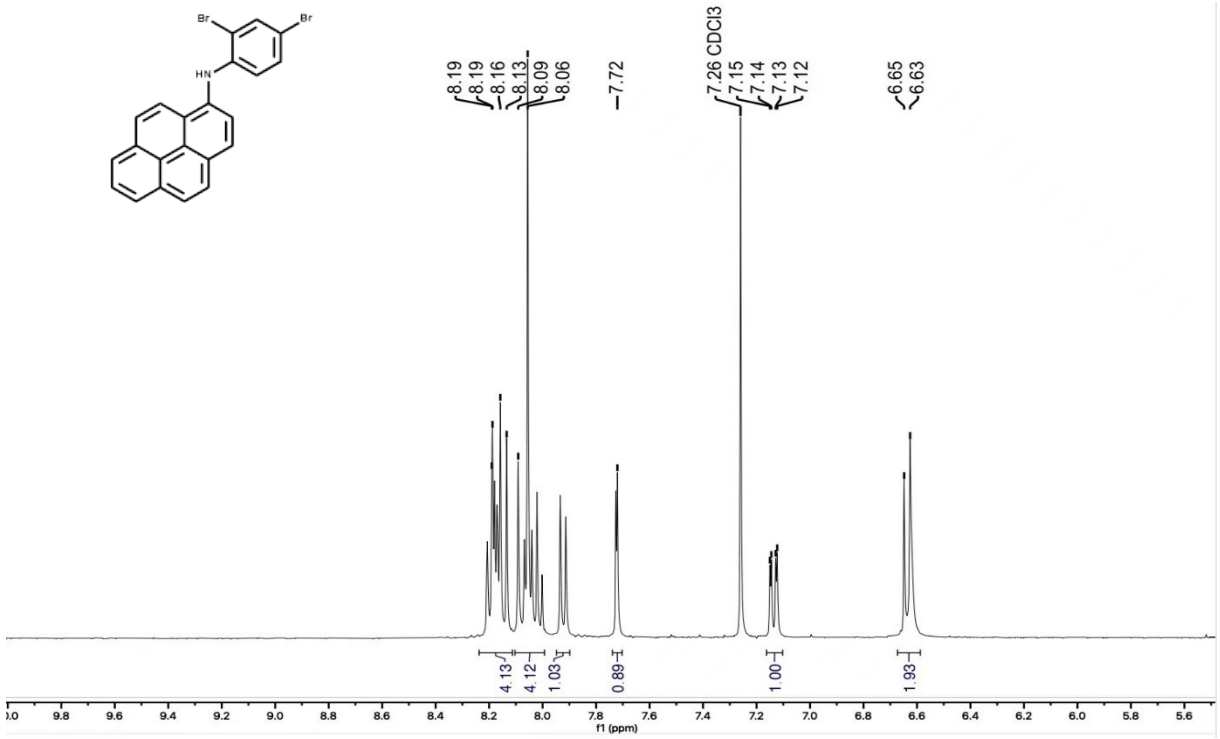

Figure S4. ^{1}H NMR spectrum of N-(2,4-dibromophenyl)pyren-1-amine in Chloroform-*d*.

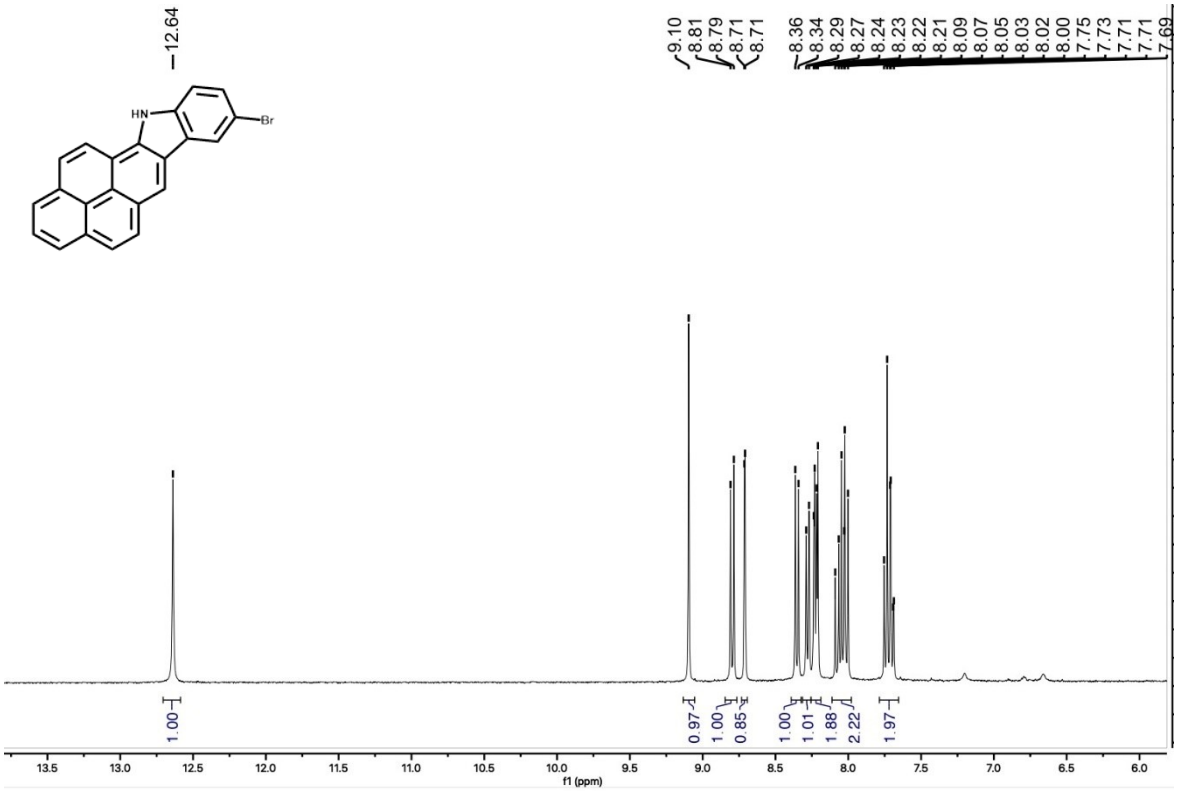

Figure S5. ^{1}H NMR spectrum of BrPyCz in DMSO-d_6.

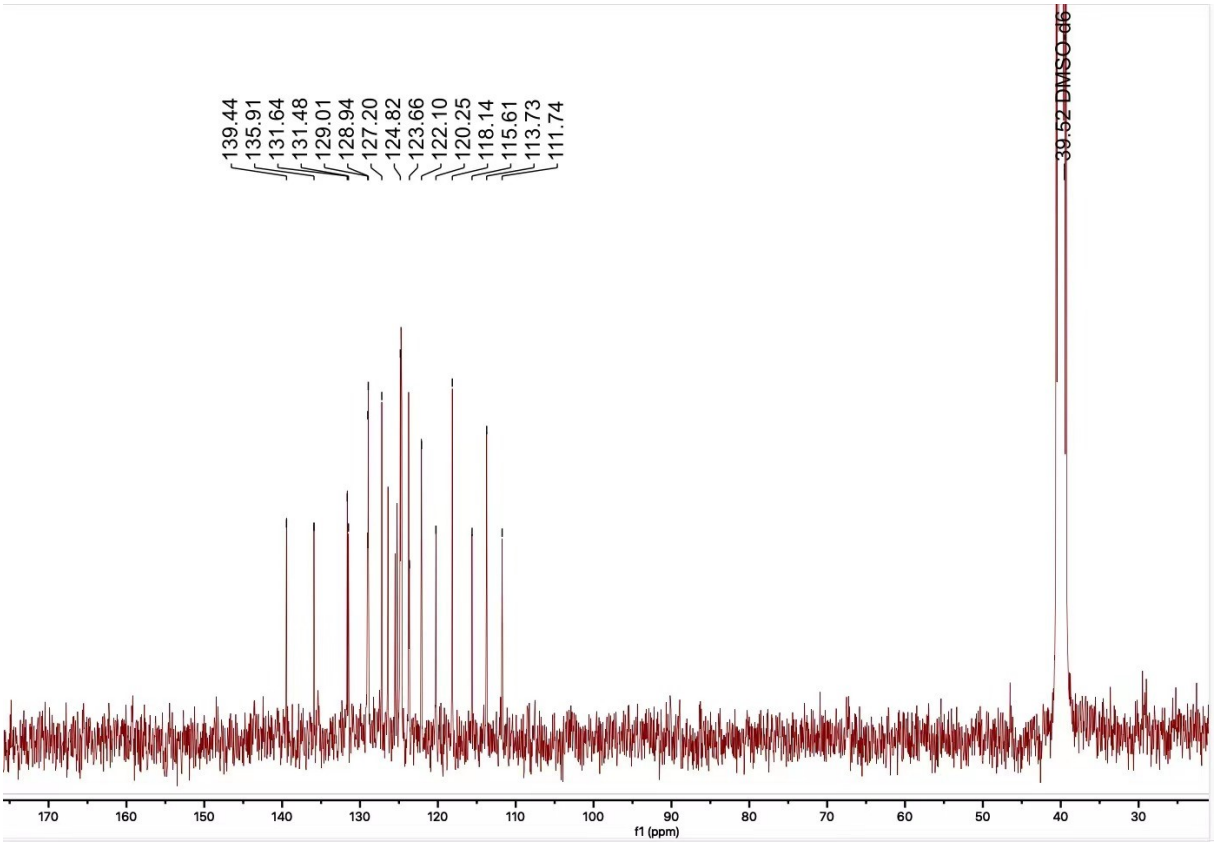

Figure S6. ^{13}C NMR spectrum of BrPyCz in DMSO-d_6.

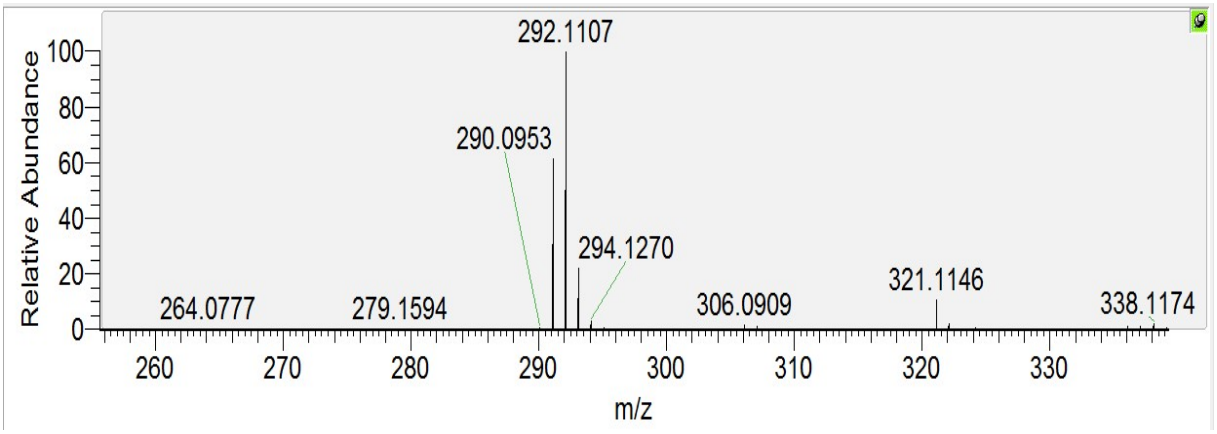

Figure S7. HR-MS spectrum of PyCz.

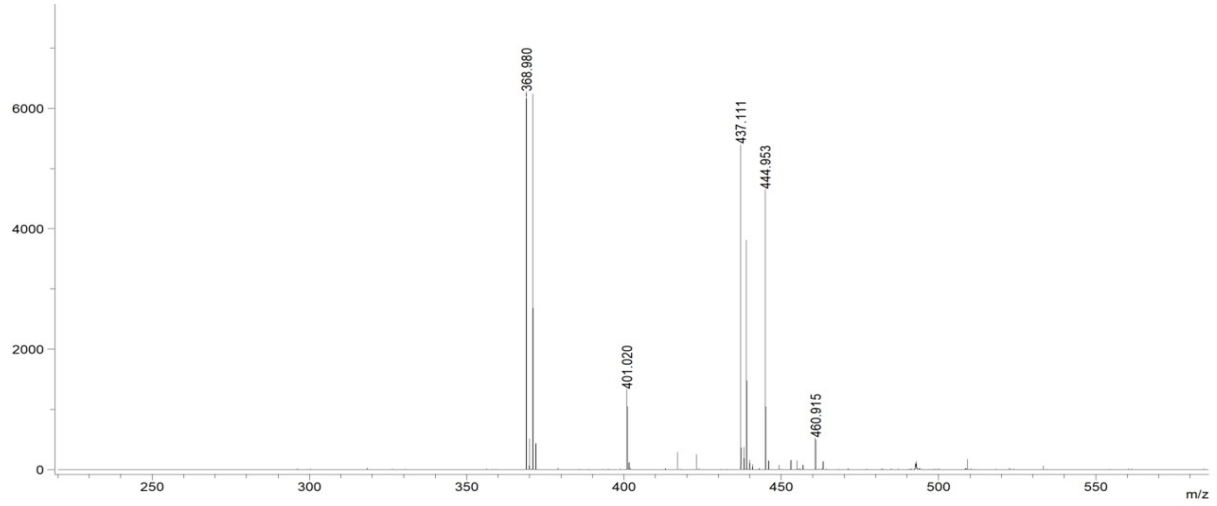

Figure S8. HR-MS spectrum of BrPyCz.

4. Photophysical properties in the solution

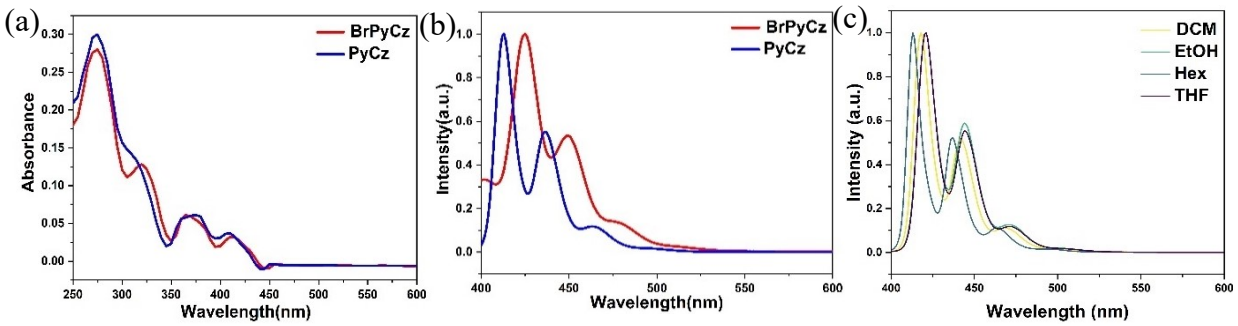

Figure S9. (a) Absorption spectra of PyCz and BrPyCz in THF solution. (b) PL spectra of PyCz and BrPyCz in THF solution and (c) PyCz in dilute solution. (20 μM, λex = 365 nm)

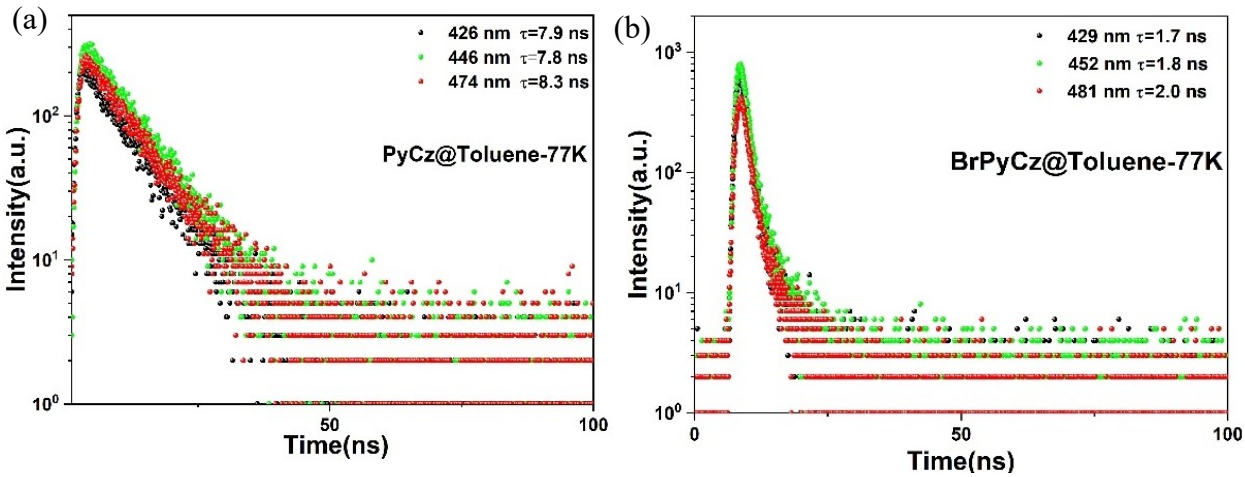

Figure S10. Decay spectra of (a) PyCz and (b) BrPyCz toluene solution at 77K. (λex = 365 nm)

5. Photophysical properties in the solid state

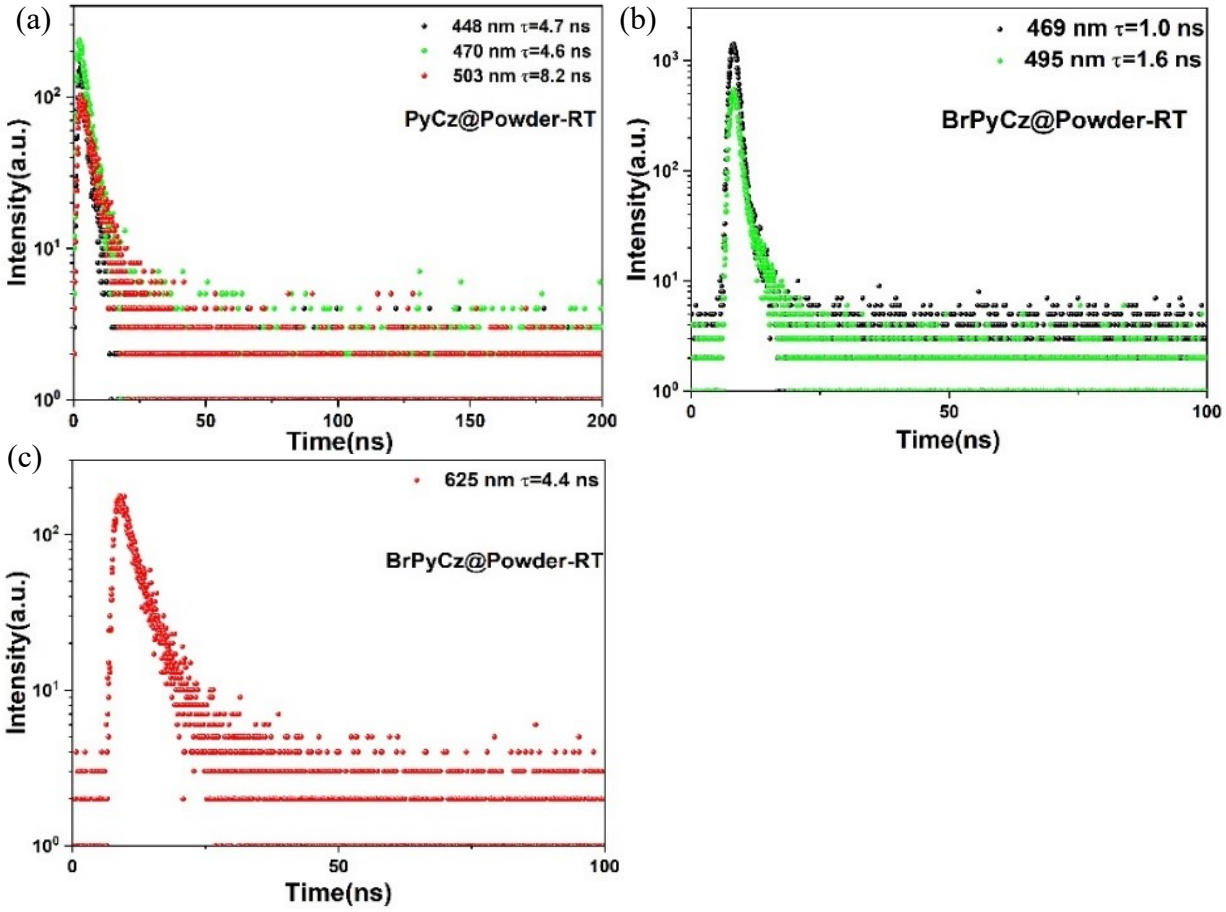

Figure S11. Decay spectra of (a) PyCz and (b) BrPyCz powder at room temperature. (λex = 365 nm)

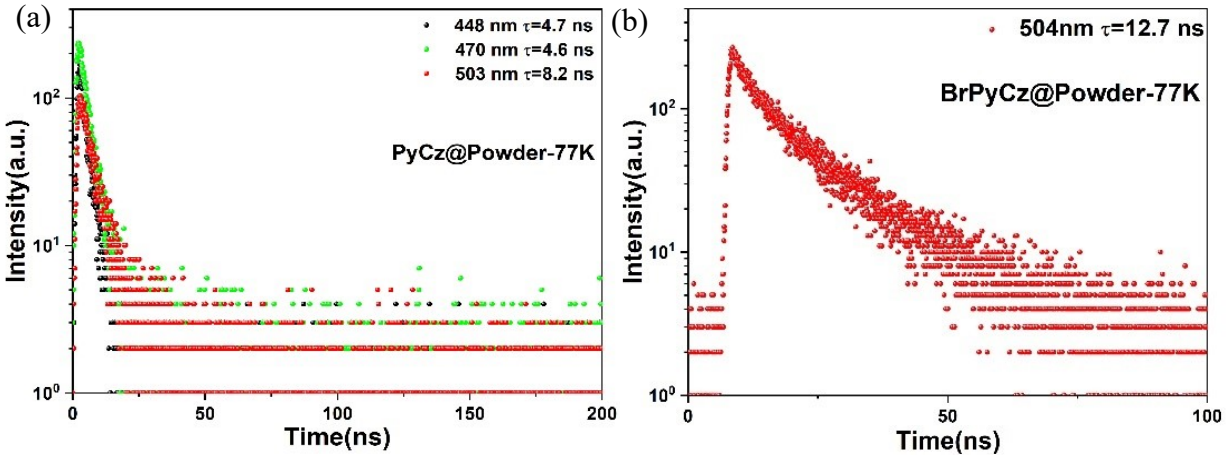

Figure S12. Decay spectra of (a) PyCz and (b) BrPyCz powder at 77 K. (λex = 365 nm)

6. Photophysical properties in the PMMA film.

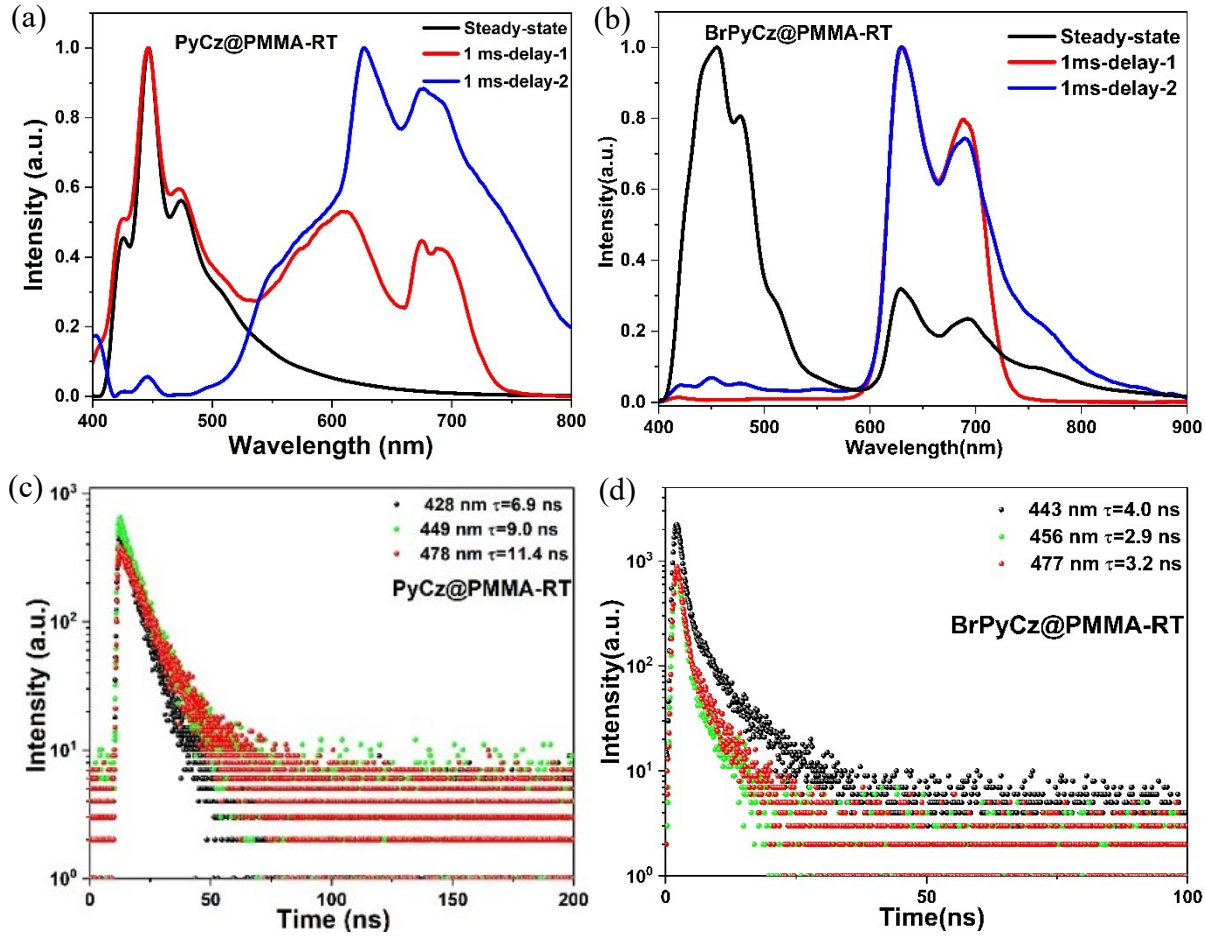

Figure S13. Steady-state and delayed PL spectra of (a) PyCz and (b) BrPyCz@PMMA film (1 wt%) at room temperature. Decay spectra of (c) PyCz and (d) BrPyCz@PMMA at room temperature. (λex = 365 nm)

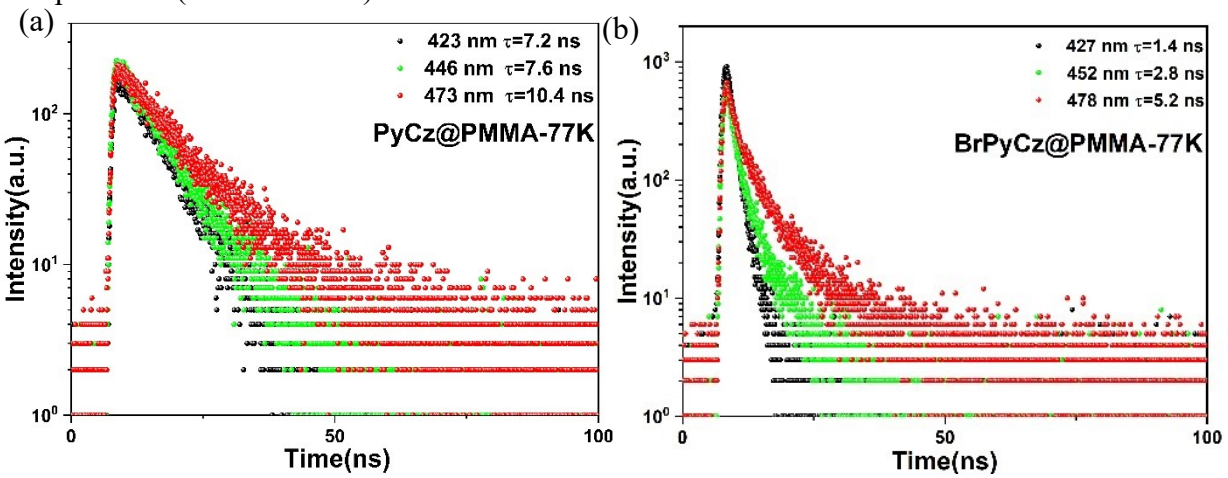

Figure S14. Decay spectra of (a) PyCz and (b) BrPyCz@PMMA (1 wt%) at 77 K. (λex = 365 nm)

7. Photophysical properties in the PVA film.

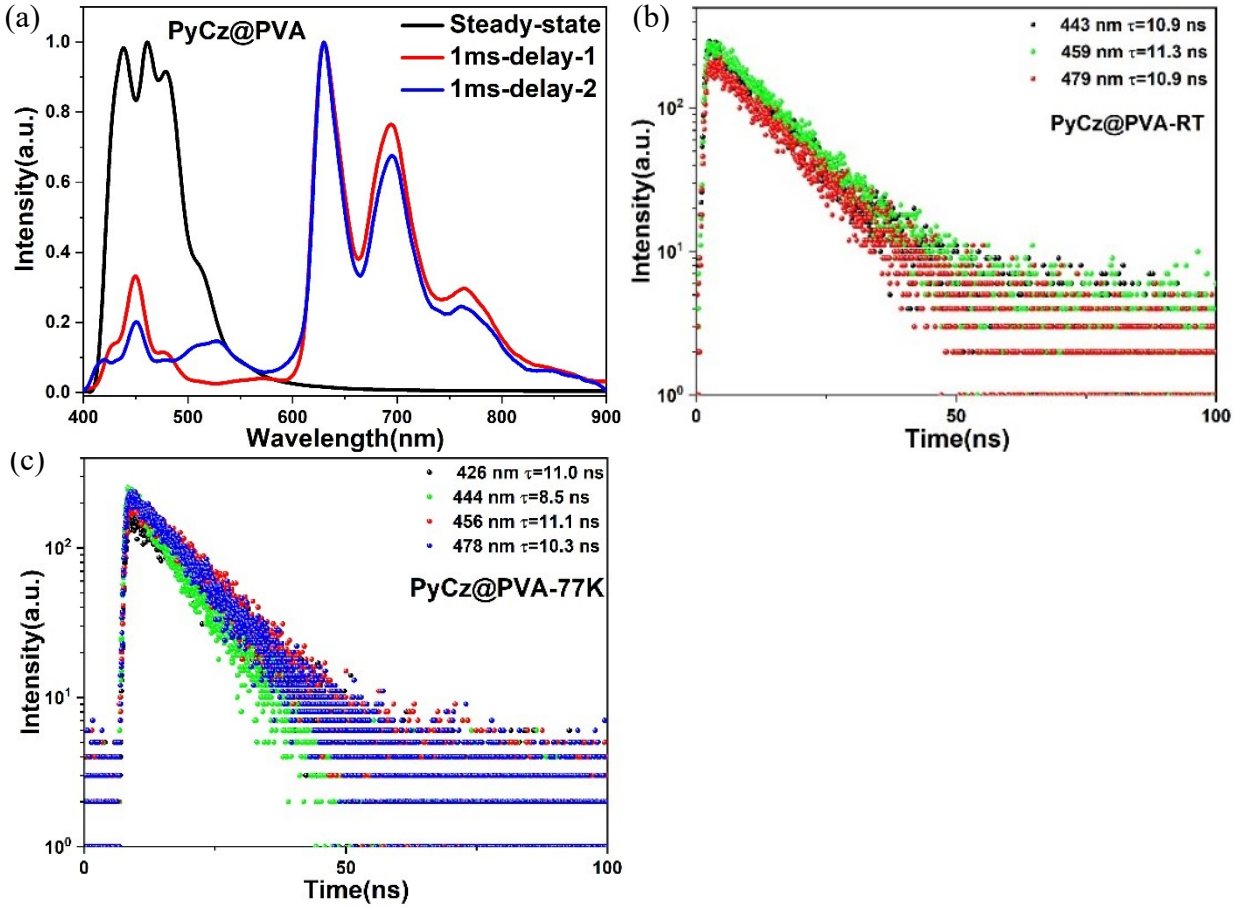

Figure S15. (a) Steady-state and delayed PL spectra of PyCz@PVA film (0.1 wt%) at room temperature. Decay spectra of PyCz@PVA at (b) room temperature and (c) 77 K. (λex = 365 nm)

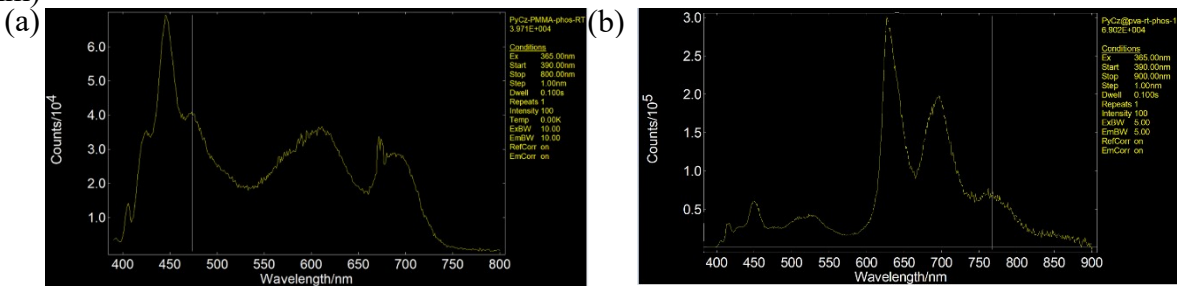

Figure S16. 1 ms delay PL spectra of (a) the PyCz@PMMA film (1 wt%) and (b) the PyCz@PVA film (0.1 wt%) at room temperature.

8. PLQY values of different films.

Table S1. PLQY values of PyCz and BrPyCz in PMMA and PVA films.

Sample	λ_{ex}/nm	φ_{PL}/%
PyCz@PMMA	365	0.04
BrPyCz@PMMA	365	0.23
PyCz@PVA	365	0.99

9. Photophysical properties of different phosphorescence units

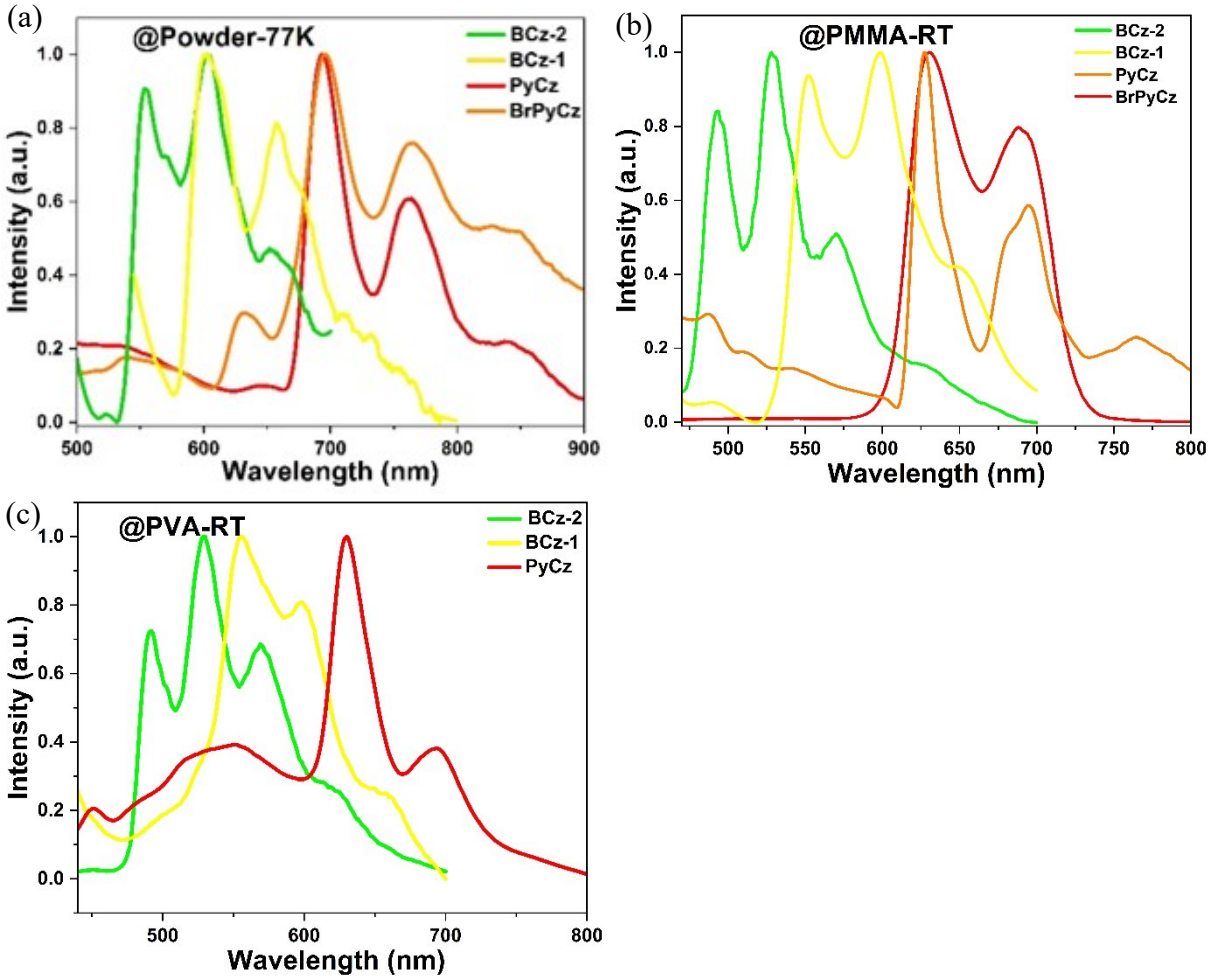

Figure S17. Delayed PL spectra of BCz-1, BCz-2, PyCz and BrPyCz (a) powders at 77 K; (b) in PMMA film (1 wt%) and (c) in PVA film (0.1 wt%) at room temperature. (λex = 365 nm)

10. Data table of the single crystal

Table S2. Detailed data of the PyCz single crystal.

Identification code	PyCz
CCDC Number	2269749
Empirical formula	C22H13N
Formula weight	291.33
Temperature	115.6(2)
Crystal system	tetragonal
Space group	$I4_1cd$
Unit cell dimensions	a= 7.2243(3), α= 90.00°
	b= 7.2243(3), β= 90.00°
	c= 53.138(5), γ= 90.00°
Volume	2773.3(3) $Å^3$
Z	8
Density (calculated)	1.396 Mg/m^3
Absorption coefficient	0.081 mm^{-1}
F(000)	1216
Crystal size	0.36 × 0.35 × 0.08 mm^3
Theta range for data collection	8.12 to 52°
Index ranges	-8≤h≤8, -8≤k≤8, -65≤l≤65
Reflections collected	10613
Independent reflections	1355 [R(int) = 0.0561(inf-0.9 Å)]
Final R indices [I>2sigma(I)]	R1 = 0.1808, wR2 = 0.4853
R indices (all data)	R1 = 0.2080, wR2 = 0.5141

11. TD-DFT results

Table S3. The singlet and triplet excited state transition configurations of BrPyCz monomer. The matched excited states that contain the same orbital transition components of S_1 are shown in bold.

Excited State	Energy(eV)	Transition configuration(%)
T_1	2.0259	H-2→L(3.68), H-1→L+1(2.16), H→L(86.13), H→L+1(4.56)
T_2	2.8628	H→L(7.13), H→L+1(83.93)
T_3	3.0988	H-2→L(3.19), H-2→L+1(2.83), H-1→L(71.29), H-1→L+1(8.44), H→L+1(2.10)
S_1	**3.1386**	**H-1→L+1(4.06), H→L(74.65), H→L+1(15.67)**
S_2	3.3517	H-1→L(23.15), H→L(16.03), H→L+1(57.54)
T_4	3.4035	H-4→L(5.57), H-3→L(11.62), H→L+2(58.87), H→L+4(10.60)

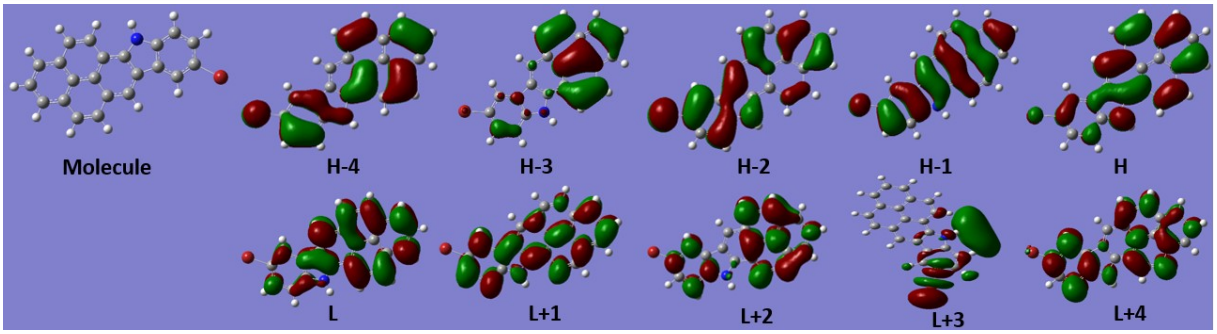

Figure S18. Plots of BrPyCz monomer visualized orbitals.

Table S4. The singlet and triplet excited state transition configurations of PyCz monomer.The matched excited states that contain the same orbital transition components of S_1 are shown in bold.

Excited State	Energy(eV)	Transition configuration(%)
T_1	2.0295	H-2→L(3.10), H-1→L+1(2.02), H→L(88.18), H→L+1(2.77)
T_2	2.9220	H-1→L+1(2.95), H→L(4.97), H→L+1(85.91)
T_3	3.0876	H-1→L(76.70), H-1→L+1(9.47), H→L+1(2.91)
S_1	**3.1706**	**H-1→L(2.97), H-1→L+1(5.33), H→L(76.79), H→L+1(12.06)**
S_2	3.3684	H-1→L(26.83), H→L(13.49), H→L+1(56.10)
T_4	3.3995	H-4→L(5.35), H-3→L(11.63), H-2→L+2(2.01), H→L+2(66.65), H→L+4(5.64)

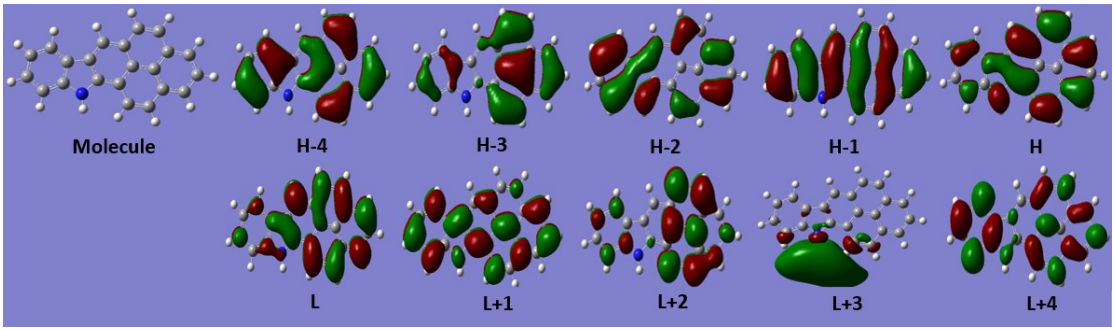

Figure S19. Plots of PyCz monomer visualized orbitals.

Table S5. The singlet and triplet excited state transition configurations of BCz-1 monomer. The matched excited states that contain the same orbital transition components of S_1 are shown in bold.

Excited State	Energy(eV)	Transition configuration(%)
T_1	2.3207	H-2→L(2.15), H-1→L(4.82), H→L(84.43), H→L+1(3.61)
T_2	3.1346	H-1→L(80.62), H-1→L+1(2.56), H→L(6.98)
S_1	**3.3441**	**H-1→L(2.10), H→L(93.68)**
T_3	3.4694	H-2→L(24.17), H-1→L(2.70), H→L(5.03), H→L+1(53.81), H→L+4(5.36)

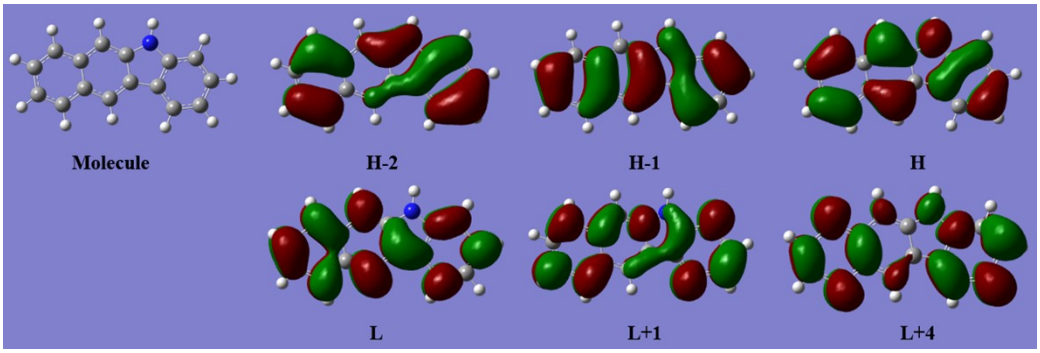

Figure S20. Plots of BCz-1 monomer visualized orbitals.

Table S6. The singlet and triplet excited state transition configurations of BCz-2 monomer. The matched excited states that contain the same orbital transition components of S_1 are shown in bold.

Excited State	Energy (eV)	Transition configuration (%)
T_1	2.6101	H-1→L (6.30), H→L (81.95)
T_2	3.1996	H-2→L (3.33), H-2→L+2 (2.49), H-1→L (75.23), H→L (8.95), H→L+1 (2.03) , H→L+2 (2.62)
T_3	3.5629	H-3→L (19.26), H-2→L (4.15), H-1→L (10.69), H-1→L+4 (4.23), H→L+1 (35.36) , H→L+2 (15.78)
S_1	**3.6645**	**H-1→L (10.03), H-1→L+1 (3.45), H→L (82.29)**
T_4	3.8392	H-3→L (8.71), H-3→L+1 (4.11), H-2→L (4.29), H-1→L+1 (9.37), H-1→L+2 (10.72) , H-1→L+4 (2.74), H→L (5.33), H→L+1 (25.53) , H→L+2 (19.58)
S_2	3.8957	H-1→L (72.47), H→L (11.10), H→L+1 (13.56)

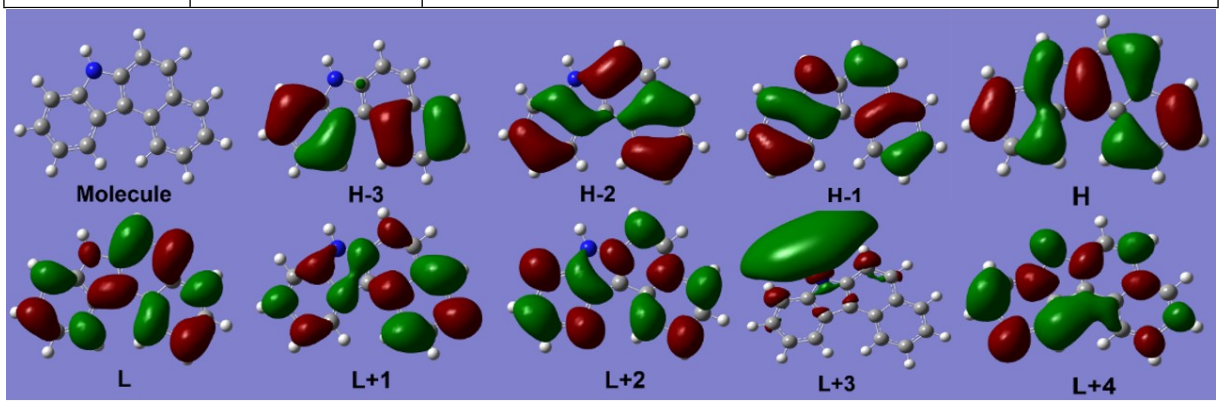

Figure S21. Plots of BCz-2 monomer visualized orbitals.

Table S7. Spin-orbit coupling (SOC) values between S_n and T_n of BrPyCz, PyCz, BCz-1 and BCz-2 monomer.

$<S_n\|Hso\|T_n>$	BrPyCz (cm^{-1})	PyCz (cm^{-1})	BCz-1 (cm^{-1})	BCz-2 (cm^{-1})
S_0/T_1	10.05269	0.11535	0.13601	0.07170
S_0/T_2	56.99668	0.10551	0.11931	0.09041
S_0/T_3	26.31901	0.15365	0.51951	0.79718
S_0/T_4	30.22747	1.37382	0.42142	-
S_1/T_1	2.19724	0.81869	0.51703	0.84868
S_1/T_2	3.15753	1.05844	0.94130	0.80073
S_1/T_3	6.14251	0.80222	0.32758	0.15102
S_1/T_4	1.37120	0.02609	0.41578	-

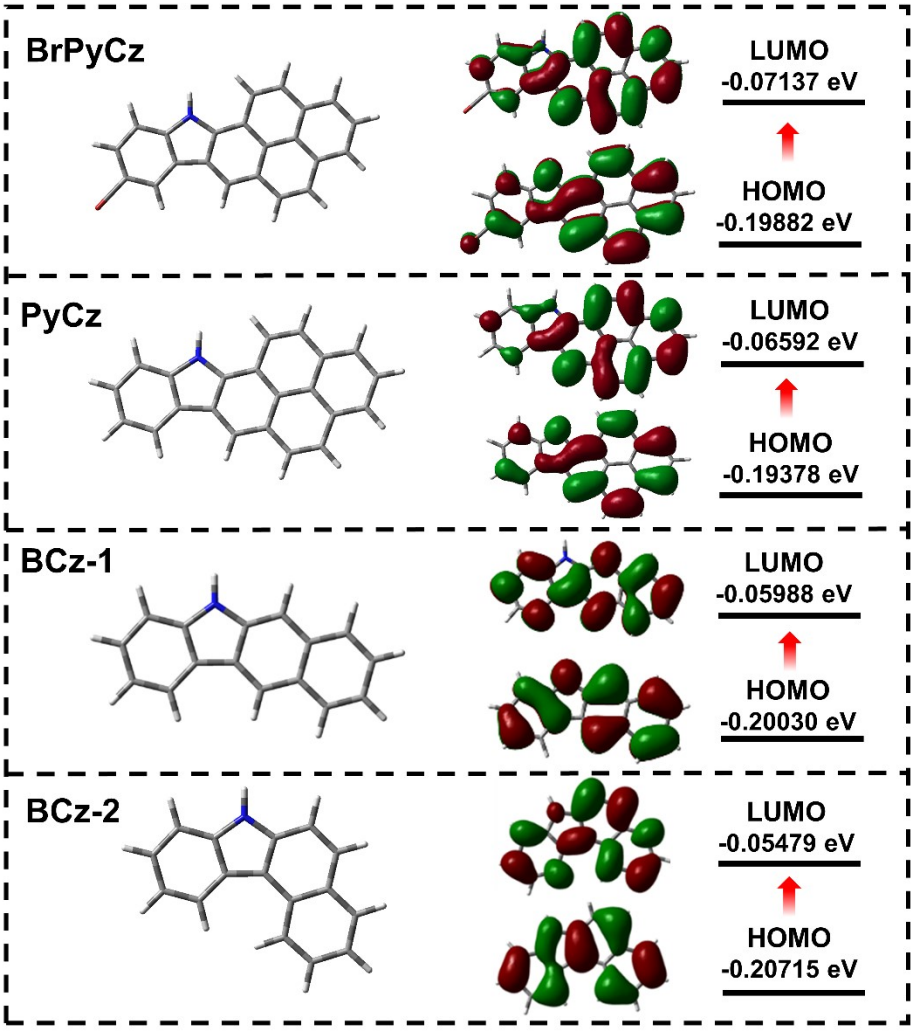

Figure S22. Plots of BrPyCz, PyCz, BCz-1 and BCz-2 monomer visualized orbitals.

Referrences

(1) M. J. Frisch, G. W. Trucks, H. B. Schlegel, G. E. Scuseria, M. A. Robb, J. R. Cheeseman, G. Scalmani, V. Barone, G. A. Petersson, H. Nakatsuji, X. Li, M. Caricato, A. V. Marenich, J. Bloino, B. G. Janesko, R. Gomperts, B. Mennucci, H. P. Hratchian, J. V. Ortiz, A. F. Izmaylov, J. L. Sonnenberg, Williams, F. Ding, F. Lipparini, F. Egidi, J. Goings, B. Peng, A. Petrone, T. Henderson, D. Ranasinghe, V. G. Zakrzewski, J. Gao, N. Rega, G. Zheng, W. Liang, M. Hada, M. Ehara, K. Toyota, R. Fukuda, J. Hasegawa, M. Ishida, T. Nakajima, Y. Honda, O. Kitao, H. Nakai, T. Vreven, K. Throssell, J. A. Montgomery Jr, J. E. Peralta, F. Ogliaro, M. J. Bearpark, J. J. Heyd, E. N. Brothers, K. N. Kudin, V. N. Staroverov, T. A. Keith, R. Kobayashi, J. Normand, K. Raghavachari, A. P. Rendell, J. C. Burant, S. S. Iyengar, J. Tomasi, M. Cossi, J. M. Millam, M. Klene, C. Adamo, R. Cammi, J. W. Ochterski, R. L. Martin, K. Morokuma, O. Farkas, J. B. Foresman, D. J. Fox, Wallingford, CT %. Gaussian 16, 2016.

(2) Z. An, C. Zheng, Y. Tao, R. Chen, H. Shi, T. Chen, Z. Wang, H. Li, R. Deng, X. Liu, W. Huang, *Nat. Mater.* **2015,** *14*, 685-690.

(3) X. Fu, X. Zhang,C. Qian, Z. Ma, Z. Li, H. Jiang, Z. Ma., *Chem. Mater.* **2023**, *35*, 347-357.

(4) C. Qian, X. Zhang, Z. Ma, X. Fu, Z. Li, H. Jin, M. Chen, H. Jiang, Z. Ma. **2023**, https://doi.org/10.31635/ccschem.023.202202561.